DESY 08-109
MZ-TH/09-15

DESY 08–109
MZ-TH/09–15
May 2009

ISSN 0418–9833

Inclusive D^*-meson production in ep scattering at low Q^2 in the GM-VFN scheme at NLO

G. Kramer[1] and H. Spiesberger[2]

[1] II. Institut für Theoretische Physik, Universität Hamburg,
Luruper Chaussee 149, D-22761 Hamburg, Germany

[2] Institut für Physik, Johannes-Gutenberg-Universität,
Staudinger Weg 7, D-55099 Mainz, Germany

arXiv:0906.2533v1 [hep-ph] 15 Jun 2009

Abstract

We have calculated the next-to-leading order cross sections for the inclusive production of D^*-mesons in ep collisions at HERA for finite, although very small Q^2. In this Q^2-range, the same approximations as for photoproduction can be used. Our calculation is performed in the general-mass variable-flavour-number scheme. In this approach, large logarithms of the charm transverse momentum are resummed and finite terms depending on m^2/p_T^2 are kept in the hard scattering cross sections. The theoretical results are compared with recent data from the ZEUS collaboration at HERA. On average, we find good agreement.

1 Introduction

The understanding of the dynamics of charm quark production at HERA has been improved considerably over the last ten years by the H1 and ZEUS collaborations, who have performed many measurements of inclusive D^*-meson production in the photoproduction mode of ep collisions with almost vanishing virtuality ($Q^2 \simeq 0$) of the exchanged photon, as well as in the deep-inelastic (DIS) mode (with photon virtuality $Q^2 > 0$). The theoretical description of heavy quark production in the framework of perturbative QCD is complicated due to the presence of several large scales appearing in this process. In DIS, Q^2 is large, but also the transverse momentum p_T of the produced D^*-meson may be large. In addition, depending on the kinematic range considered, also the mass m of the charm quark may have to be taken into account. Different calculational schemes have been developed which can be applied for an interpretation of experimental data, depending on the specific kinematical region and the relative importance of these three scales.

In the case of relatively small transverse momentum, $p_T \lesssim m$, the fixed-flavour number scheme (FFNS) is usually applied. Here one assumes that the light quarks (u, d, s) and the gluon are the only active flavours within the proton and the photon. In this scheme cross sections for $e + p \to e' + D^* + X$ have been calculated for DIS in Ref. [1] and for photoproduction in Ref. [2]. In photoproduction, where $Q^2 \simeq 0$, the direct process has to be supplemented with the resolved process, where the photon acts as a source of partons which interact with partons in the proton. These two interaction modes are needed to describe the singular region at $Q^2 = 0$ for massless quarks appropriately. In the FFN scheme [1, 2] the charm quark appears only in the final state of the direct and resolved processes, via the hard scattering of light partons, including the photon. The charm quark mass m is explicitly taken into account together with the transverse momentum of the produced D^*-meson; this approach is therefore expected to be reliable when p_T and m are of the same order of magnitude. In the FFNS, the charm quark mass acts as a cutoff for the initial- and final-state collinear singularities and sets the scale for the perturbative calculation. The mass m is fully retained in the calculation of the hard-scattering cross sections.

In the complementary kinematical region where $p_T \gg m$, calculations are usually based on the zero-mass variable-flavour-number scheme (ZM-VFNS). This is the conventional parton model approach where the zero-mass parton approximation is applied also to the charm quark, although its mass is not small and large compared with Λ_{QCD}. In the ZM-VFNS, the charm quark acts also as an incoming parton with its own parton distribution function (PDF) in the proton and in the photon leading to additional direct and resolved contributions. Usually, charm quark PDFs and also the fragmentation functions (FFs), describing the transition $c \to D^*$, are defined at an initial scale μ_0 chosen equal to the charm mass m. Then this is the only place, where the charm mass enters in this scheme. The D^*-meson is produced by fragmentation from the charm quark produced in the hard scattering process; but also fragmentation from the light quarks and the gluon has to be

taken into account. The well-known factorization theorem provides a unique procedure for incorporating the FFs into the lowest order (LO) and next-to-leading-order (NLO) perturbative calculations. The predictions obtained in this scheme are expected to be reliable only in the region of large p_T since all terms of the order m^2/p_T^2 are neglected in the hard scattering cross section. Calculations for D^*-production in the ZM-VFNS have been performed some time ago for photoproduction in Ref. [3] and for DIS in Ref. [4].

A unified scheme that combines the virtues of the FFNS and the ZM-VFNS is the so-called general-mass variable-flavour-number scheme (GM-VFNS) [5]. In this approach the large logarithms $\ln(p_T^2/m^2)$, which appear due to the collinear mass singularities in the initial and final state, are factorized into the PDFs and FFs and summed by the well known DGLAP evolution equations [6] for the PDFs and FFs. The factorization is performed following the usual $\overline{\rm MS}$ prescription which guarantees the universality of both PDFs and FFs. At the same time, mass-dependent power corrections are retained in the hard-scattering cross sections, as in the FFNS. It is expected that this scheme is valid not only in the region $p_T^2 \gg m^2$, but also in the kinematic region where p_T is larger than a few times the charm mass m only. We should emphasize that in the GM-VFN scheme, the incorporation of the fragmentation $c \to D^*$ is based on the factorization theorem; this is a prerequisite for applying the FFs in different processes. In the usual FFNS calculation, this is not the case and non-perturbative FFs for the transition $c \to D^*$ can be supplemented on purely phenomenological grounds only.

It is the purpose of this work to present theoretical results for the D^*-production cross section in $e^{\pm}p$ scattering with finite non-zero photon virtuality in the region $0.05 < Q^2 < 0.7$ GeV^2 and discuss a comparison with experimental results obtained with the ZEUS detector at HERA [7]. We shall calculate all cross sections with the same kinematical constraints as in the ZEUS analysis [7] in the GM-VFNS. Since in the ZEUS experiment the photon virtuality is small, the application of the photoproduction approximation is justified where the Q^2-dependence in the hard scattering cross sections is neglected.

Details of our calculation have been described recently in Ref. [8]. In this work, we had also studied theoretical uncertainties of the photoproduction cross section in the GM-VFNS due to various possible choices for input variables, as for example, the proton and photon PDFs and the D^* FFs. In that reference one can also find a discussion of the dependence on the factorization and renormalization scales and the influence of the charm quark mass m. The application of the theoretical framework described there to the present case of low-Q^2 DIS is straightforward and amounts to an adjustment of the parameters entering the Weizsäcker-Williams approximation [9] for the flux of the virtual photon. Instead of $Q^2_{\rm min} = m_e^2 y^2/(1-y)$ and the value for $Q^2_{\rm max}$ given by the anti-tagging condition of the final electron (positron) as used in the measurement of the photoproduction process, we have to fix $Q^2_{\rm min}$ and $Q^2_{\rm max}$ to the values used in the ZEUS analysis. We will consider the kinematic range as in Ref. [7], i.e. $0.05 < Q^2 < 0.7$ GeV^2.

The outline of the paper is as follows. In Section 2 we give a short description of the various input options used in the calculation. Section 3 contains our results and the

comparison with the experimental data from ZEUS.

2 Input choices for the calculation

The D^*-electroproduction cross section $\sigma_{ep}(\sqrt{s})$ at the ep center-of-mass energy $\sqrt{s}$ is related to the photoproduction cross section at center-of-mass energy $W_{\gamma p}$, $\sigma_{\gamma p}(W_{\gamma p})$, in the following way:

$$\sigma_{ep}(\sqrt{s}) = \int_{y_{\min}}^{y_{\max}} dy f_{e\gamma}(y, Q^2_{\min}, Q^2_{\max}) \sigma_{\gamma p}(y\sqrt{s}) \,. \tag{1}$$

Here, $f_{e\gamma}$ is the energy spectrum of the exchanged virtual photon which in the Weizsäcker-Williams approximation [9] is given by

$$f_{e\gamma}(y, Q^2_{\min}, Q^2_{\max}) = \frac{\alpha}{2\pi} \left[\frac{1+(1-y)^2}{y} \ln \frac{Q^2_{\max}}{Q^2_{\min}} + 2 m_e y \left(\frac{1}{Q^2_{\max}} - \frac{1}{Q^2_{\min}} \right) \right] . \tag{2}$$

The photon flux $f_{e\gamma}$ depends on y, $Q^2_{\min}$ and $Q^2_{\max}$. The range of y, $y_{\min} \leq y \leq y_{\max}$, as well as the limits $Q^2_{\min}$ and $Q^2_{\max}$, are determined by the cuts and bin limits in the experimental analysis. In photoproduction, $Q^2_{\min} \propto m_e^2$ is very small, whereas in the ZEUS analysis $Q^2_{\min} = 0.05$ GeV^2 and $Q^2_{\max} = 0.7$ GeV^2, or within these limits for the measurement of the Q^2 distribution. α is the electromagnetic fine structure constant and $y = E_\gamma / E_e$, the ratio of the energies of the incoming photon and electron, is determined by the inelasticity $y = Q^2/(2P \cdot q)$ where P and q are the 4-momenta of the incoming proton and the photon.

The cross section for direct photoproduction in Eq. (1) is a convolution of the proton PDF, the fragmentation function for the transition of parton a to the observed D^*-meson (where $a = u$, $\bar{u}$, d, $\bar{d}$, s, $\bar{s}$, c, $\bar{c}$, and g) and the cross section for the hard scattering process $\gamma b \to aX$. For the resolved contribution, an additional convolution with the photon PDFs has to be performed. The hard scattering cross sections are calculated including next-to-leading order corrections of the order $O(\alpha_s)$. The PDFs are evolved at NLO. For the photon PDF we use the set GRV92 of Ref. [10], converted to the $\overline{\rm MS}$ factorization scheme; for the proton PDF we have chosen the most recent parametrization CTEQ6.6M [11] of the CTEQ group.

For the FFs we use the set Belle/CLEO-GM of Ref. [12]. Note that in our previous work [8] we had used the set Global-GM instead, where also LEP1 data [13] at large s had been included in the fit, whereas the set Belle/CLEO-GM is based on a fit of the combined Belle [14] and CLEO [15] data at $\sqrt{s} = 10.52$ GeV only. For the photoproduction cross section $d\sigma/dp_T$ we found results larger by $25-30\%$ in average when using the Belle/CLEO-GM parametrization, as compared to the set Global-GM of Ref. [12]. The strong coupling constant $\alpha_s^{(n_f)}(\mu_R)$ is evaluated with the two-loop formula [16] with $n_f = 4$ active quark flavours and the asymptotic scale parameter $\Lambda^{(4)}_{\overline{\rm MS}} = 328$ MeV, corresponding

to $\alpha_s^{(5)}(m_Z) = 0.118$. The charm quark mass is fixed to $m = 1.5$ GeV. We choose the renormalization scale μ_R and the factorization scales μ_F and $\mu_{F'}$ related to initial- and final-state singularities to be $\mu_R = \xi_R m_T$ and $\mu_F = \mu_{F'} = \xi_F m_T$, where $m_T = \sqrt{m^2 + p_T^2}$ is the transverse mass and ξ_R and ξ_F are parameters varied about their default values $\xi_R = \xi_F = 1$ in order to assess theoretical uncertainties as described below.

As already mentioned in the introduction, the photoproduction cross section is calculated in the GM-VFN scheme. In this scheme the cross section has a smooth limit for $m \to 0$ and approaches the result of the ZM-VFN scheme for $m \to 0$ or $p_T \to \infty$. The basic features of the GM-VFNS are described in Ref. [8] and the literature quoted therein. Compared to the ZM-VFNS, the GM-VFNS incorporates mass-dependent terms as in the FFNS, so that the cross sections calculated in the GM-VFNS are supposed to be valid also for medium scale p_T values, close to the heavy-quark mass. In order to conform with the $\overline{\rm MS}$ factorization of singularities, finite subtraction terms must be supplemented to the results of the FFNS calculation. These subtraction terms had been calculated in Ref. [17] for the direct photon, and in Ref. [18] for the resolved photon contributions. They include logarithmic, scale-dependent contributions related to gluon emission from charm quarks and to charm-anticharm production from incoming gluons. As a consequence, in the GM-VFNS one has to take into account also processes with incoming charm quarks, involving corresponding charm-quark components in the PDFs of the photon and the proton. In addition, for the final state, apart from the FF describing the transition $c \to D^*$, also FFs for the transition of a light parton to the heavy meson, $a \to D^*$, are needed. These contributions are not present in the FFNS calculation. Instead, they are taken into account at fixed order of perturbation theory as part of the hard scattering cross sections. Compared with the ZM- and GM-VFNS approaches, the FFNS has the advantage that it is valid also for $0 < p_T \lesssim m$, a property which is not realized in the presently available implementation of the GM-VFNS. A reliable prediction down to $p_T = 0$ is necessary if total cross sections for heavy-meson production are to be calculated.

In our calculation we implement the experimental conditions of the ZEUS analysis: the energies of the incoming protons and electrons (positrons) are $E_p = 920$ GeV and $E_e = 27.5$ GeV, respectively. The inelasticity y varies in the range $0.02 < y < 0.85$. The transverse momentum p_T and the rapidity η of the D^*-meson have been measured in the kinematic ranges $1.5 < p_T < 9.0$ GeV and $|\eta| < 1.5$. The photon virtuality is taken in the interval $0.05 < Q^2 < 0.7$ GeV^2.

3 Results

In this section we present our results for the differential cross sections of the process $e+p \to e'+D^*+X$ in the GM-VFNS as a function of Q^2, y, p_T and η. We choose bins in accordance with the ZEUS measurement and differential cross sections are obtained by averaging over the bin sizes as are the experimental ones [7]. The numerical results are shown in Fig. 1. We have estimated theoretical uncertainties by varying independently the parameters ξ_R

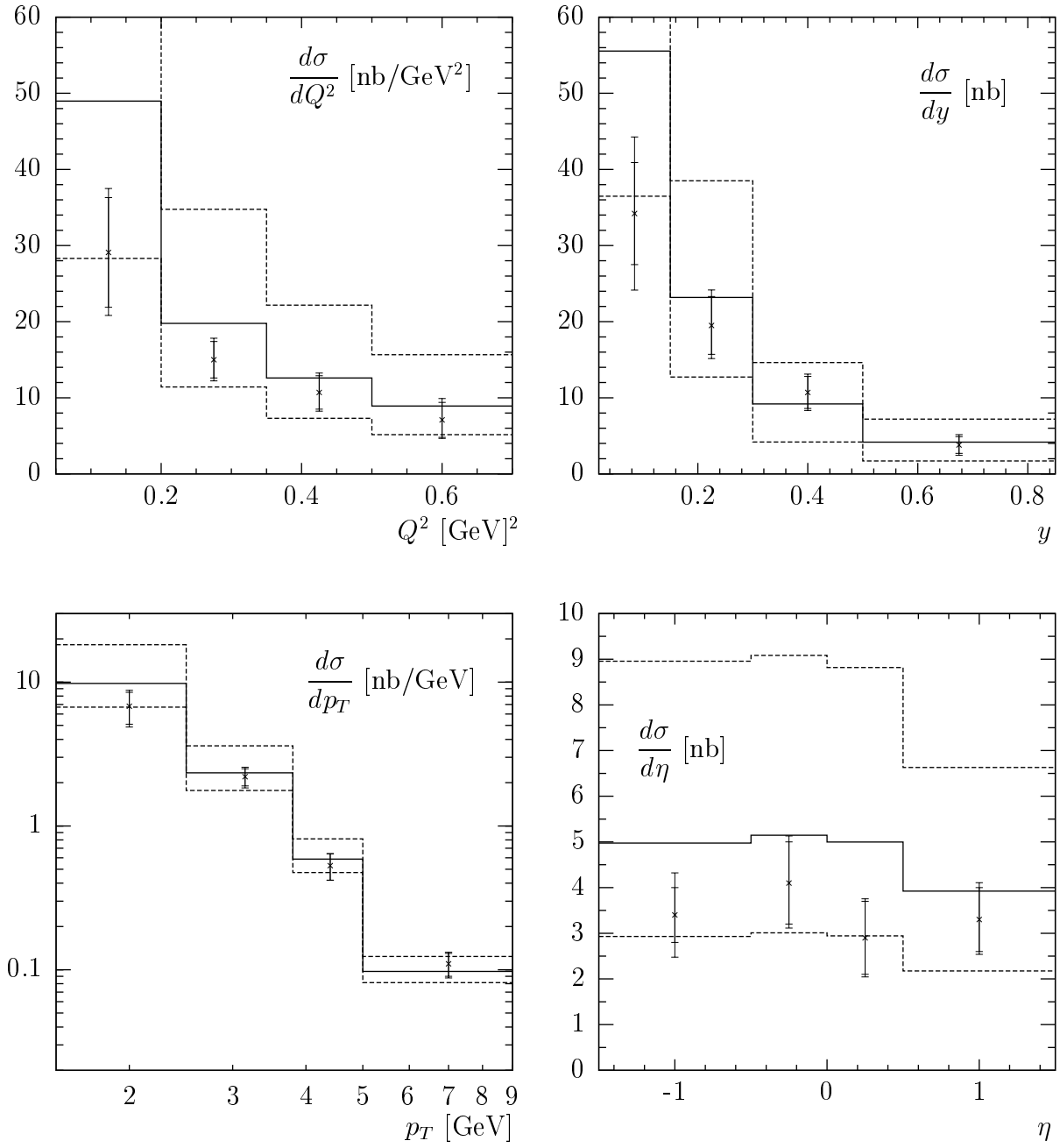

Figure 1: Differential cross sections for D^*-meson production in low-Q^2 ep scattering, compared with experimental results from the ZEUS collaboration [7]. The default choice for the scale parameters is $\xi_R = \xi_F = 1$ (full lines) and error bands are obtained by varying ξ_R and ξ_F (see text, dashed lines). The kinematic range is given by $0.05 < Q^2 < 0.7\,\mathrm{GeV}^2$, $0.02 < y < 0.85$, $1.5 < p_T < 9.0$ GeV and $|\eta| < 1.5$.

and ξ_F in the range $0.5 \leq \xi_R, \xi_F \leq 2$ about their default values $\xi_R = \xi_F = 1$ imposing the constraint $0.5 \leq \xi_F/\xi_R \leq 2$. The maximal and minimal differential cross sections obtained

this way are shown in Fig. 1 as dashed lines together with the central values (full lines). Comparing the errors of the ZEUS data points and the theoretical errors due to the scale variation we observe that all data points for $d\sigma/dQ^2$, $d\sigma/dy$, $d\sigma/dp_T$ and $d\sigma/d\eta$ are compatible with our theoretical predictions. Most of the predictions with the default scale choice $\xi_R = \xi_F = 1$ are found inside the range given by the data and their experimental errors. The discrepancies between theoretical prediction and experimental measurement are largest for the smallest values of Q^2, p_T and y; however, also the theoretical error band is largest for these bins. Since small values of these kinematic variables dominate at all values of η, the uncertainty due to scale variations is large for all bins of $d\sigma/d\eta$. For $d\sigma/dp_T$ the relative size of the error band decreases with increasing p_T, as expected. In the first bin of the p_T distribution where $p_T(\mathrm{min}) \simeq 1.5$ GeV, the scale variable μ_F is small, approximately equal to $1.5 \times m$, which explains the large sensitivity to scale variations.

Actually we can not expect our theoretical framework to be particularly accurate at small p_T, close to $p_T \simeq m$, since the cross section in the GM-VFNS contains parts which are calculated in the massless approximation. This prevents us to calculate cross sections down to $p_T = 0$ and consequently also the total D^*-production cross section integrated over p_T can not be calculated reliably. In the kinematic region $p_T \lesssim m$, the FFNS is the better choice. The comparison of the data in the first p_T bin with the FMNR result for photoproduction [2], as presented in Ref. [7], shows indeed good agreement. Since $d\sigma/dp_T$ is over-estimated in our approach for $p_T \simeq m$, also the cross section integrated over the full range of p_T values considered in the ZEUS experimental analysis is too large: the measured total cross section quoted in Ref. [7] is[1] $\sigma(ep \to e'D^*X) = 10.1^{+1.5}_{-1.3}$ nb, whereas the corresponding theoretical prediction is $13.9^{+10.4}_{-5.8}$ nb. In the restricted p_T-range $2.5 \leq p_T \leq 9$ GeV, we find instead $4.1^{+2.0}_{-0.9}$ nb to be compared with the experimental value of 3.9 ± 0.4 nb (obtained from the results given in [7] by summing over the last three p_T bins), i.e. for larger p_T the theoretical cross section in the GM-VFNS agrees with the measured one quite well.

In obtaining theoretical predictions for the photoproduction cross section, one has to distinguish direct and resolved components. Each of the two parts depends on the choice of a factorization scheme and can not be compared separately to experimental data. Only the sum of the direct and resolved contributions has a physical meaning. From the theoretical point of view, it is nevertheless interesting to study the decomposition of the cross section into these two components, in particular in view of a comparison with results obtained in the FFNS approach for photoproduction [2] or for DIS [1]. In DIS at large Q^2, there is only a direct contribution to the cross section since initial-state singularities appearing in the limit $Q^2 \to 0$ have not to be subtracted. The photoproduction cross section in the FFN scheme [2] has a smaller resolved part than in the GM-VFNS, since it originates only from initial gluons and light quarks, whereas in the GM-VFNS also processes with charm quarks in the initial state contribute. Therefore, in our case the

[1] Statistical and systematic errors, and an error due to the uncertainty in the branching ratios, are added in quadrature.

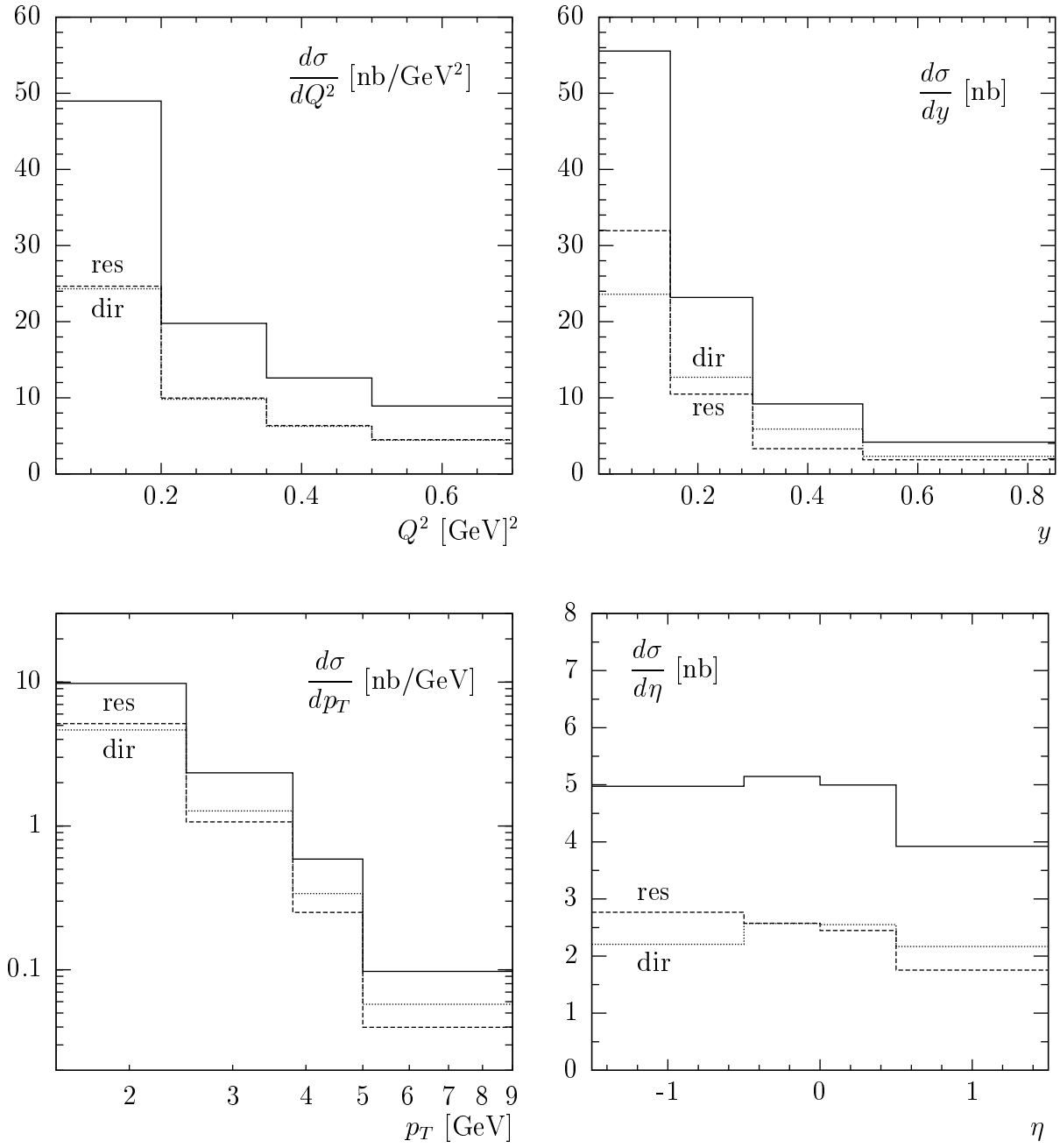

Figure 2: Differential cross sections for D^*-meson production in low-Q^2 ep scattering in the kinematic range $0.05 < Q^2 < 0.7$ GeV^2, $0.02 < y < 0.85$, $1.5 < p_T < 9.0$ GeV, $|\eta| < 1.5$. The full cross section (full lines) is separated into its direct (dotted lines) and resolved parts (dashed lines) for $\xi_R = \xi_F = 1$.

direct and resolved contributions are of comparable magnitude. This is seen in detail in Fig. 2 where we have plotted these two components and their sum for $d\sigma/dQ^2$, $d\sigma/dy$, $d\sigma/dp_T$ and $d\sigma/d\eta$.

We conclude that in the general-mass variable-flavour-number scheme, the photoproduction approximation, i.e. the approximation where the hard scattering cross sections are evaluated with $Q^2 = 0$, leads to theoretical predictions in very good agreement with recent ZEUS data for finite, but small $Q^2 \neq 0$, in particular for the larger values of p_T. The description of the measurement at the smallest values of $p_T \simeq 1.5$ GeV is less satisfactory, but still in agreement with data within errors.

References

[1] B. W. Harris and J. Smith, Phys. Rev. D57 (1998) 2806; and earlier references given there.

[2] S. Frixione, M. Mangano, P. Nason and G. Ridolfi, Phys. Lett. B 348 (1995) 633; S. Frixione, P. Nason and G. Ridolfi, Nucl. Phys. B 545 (1995) 3; and earlier references given there.

[3] J. Binnewies, B. A. Kniehl and G. Kramer, Phys. Rev. D58 (1998) 014014; Z. Phys. C76 (1997) 677; B. A. Kniehl, G. Kramer and M. Spira, Z. Phys. C76 (1997) 689; M. Cacciari and M. Greco, Z. Phys. C69 (1996) 459; Phys. Rev. D55 (1997) 7134.

[4] I. Schienbein, Proc. of the Ringberg Workshop "New Trends in HERA Physics 2005", eds. G. Grindhammer et al., World Scientific Publishing, Singapore 2006 [hep-ph/0601235]. A comparison with H1 data is shown in A. Aktas et al., H1 Collaboration, Eur. Phys. J. C51 (2007) 271.

[5] G. Kramer and H. Spiesberger, Eur. Phys. J. C38 (2004) 309; B. A. Kniehl, G. Kramer, I. Schienbein and H. Spiesberger, Phys. Rev. D71 (2005) 014018.

[6] V. N. Gribov and L. N. Lipatov, Sov. J. Nucl. Phys. 15 (1972) 438 [Yad. Fiz. 15 (1972) 781]; Yu. L. Dokshitzer, Sov. Phys. JETP 46 (1977) 641 [Zh. Eksp. Theor. Fiz. 73 (1977) 1216]; G. Altarelli and G. Parisi, Nucl. Phys. B126 (1977) 298.

[7] ZEUS Collaboration, S. Chekanov et al., Phys. Lett. B649 (2007) 111.

[8] B. A. Kniehl, G. Kramer, I. Schienbein and H. Spiesberger, arXiv:0902.3166 [hep-ph], Eur. Phys. J. C (to be published).

[9] C. F. von Weizsäcker, Z. Phys 88 (1934) 612; E. J. Williams, Phys. Rev. 45 (1934) 729; P. Kessler, Acta Phys. Austriaca 41 (1975) 141; S. Frixione, M. L. Mangano, P. Nason and G. Ridolfi, Phys. Lett. B319 (1993) 339.

[10] M. Glück, E. Reya and A. Vogt, Phys. Rev. D46 (1992) 1973.

[11] CTEQ Collaboration, P. M. Nadolsky et al., Phys. Rev. D78 (2008) 013004.

[12] T. Kneesch, B. A. Kniehl, G. Kramer and I. Schienbein, Nucl. Phys. B799 (2008) 34.

[13] ALEPH Collaboration, R. Barate et al., Eur. Phys. J. C16 (2000) 597; OPAL Collaboration, G. Alexander et al., Z. Phys. C72 (1996) 1; OPAL Collaboration, K. Ackerstaff et al., Eur. Phys. J. C1 (1998) 439.

[14] Belle Collaboration, R. Seuster et al., Phys. Rev. D73 (2006) 032002.

[15] CLEO Collaboration, M. Artuso et al., Phys. Rev. D70 (2004) 112001.

[16] C. Amsler et al., Particle Data Group, Phys. Lett. B667 (2008) 1.

[17] G. Kramer and H. Spiesberger, Eur. Phys. J. C22 (2001) 289; Eur. Phys. J. C28 (2003) 495.

[18] B. A. Kniehl, G. Kramer, I. Schienbein and H. Spiesberger, Phys. Rev. D 71 (2005) 014018; Eur. Phys. J. C41 (2005) 199.